

Method to generate isolated attosecond pulses with many-cycle laser fields

Songsong Tang and Xianfeng Chen*

Department of Physics, State Key Laboratory on Fiber Optic Local Area Communication Networks and Advanced Optical Communication Systems, Shanghai Jiao Tong University, Shanghai 200240, China

(Received 13 February 2012; published 13 June 2012)

We propose a scheme to generate isolated attosecond (as) pulses by high-peak-power multicycle laser fields which is based on high-order harmonics generation (HHG) from a helium atom irradiated by a three-color femtosecond (fs) laser field. An infrared laser acts as the driving laser and two tunable lasers act as control fields which are used to modulate the ellipticity and amplitude of the driving field respectively. With well-chosen parameters, an isolated 100 as pulse is generated with a duration of 50 fs.

DOI: [10.1103/PhysRevA.85.063816](https://doi.org/10.1103/PhysRevA.85.063816)

PACS number(s): 42.65.Ky, 42.65.Re, 33.80.Wz

I. INTRODUCTION

The development of research on HHG and attosecond (as) pulses has recently paved the way to “attoscience” [1] for their applications in detecting and controlling the electronic dynamics at the sub-fs time scale inside atoms [2]. Currently, trains of multiple as pulses can be generated by HHG in gases with many-cycle laser pulses [3]. However, the generation of isolated pulses which should be ideal “ultrashort probes” is technically difficult because it requires few-cycle driving lasers with stable carrier-envelope phase (CEP), and so far only several laboratories in the world use such pulses [4]. The reason is that the electric fields of these pulses vary significantly from one half-cycle to the next, and in the framework of the three-step model [5,6] for HHG, the maximum of kinetic energies (cutoff energy) of an electron returning to its parent ion is clearly different for each half cycle [7].

The difference between the highest and the second highest cutoff energies [8] of different half cycles supports the extreme ultraviolet (XUV) supercontinuum to generate isolated as pulses. Thus, the highly desirable intense isolated ultrashort pulses require the strongest laser with the shortest duration. Up to now, except the approach to enlarge the power and meanwhile compress the duration of the laser system, quantum-path control by selecting one HHG emission within one half cycle of the driving field in two-color lasers also gives out an intense XUV supercontinuum by modulating the polarization [9] or amplitude [10] of high-peak-power multicycle driving pulses. Isolated few-hundred-as pulses have been produced with 25 fs pulses by using the polarization gating technique combined with the ionization dynamics and the spatial filtering provided by the three-dimensional field propagation [11] or by the generalized double-optical-gating (GDOG) method [4]. Tzallas *et al.* produced intense isolated 340 as pulses through the interferometric modulation of the ellipticity of 50-fs-long pulses [3]. Altucci *et al.* implemented an experimental scheme for the generation of single-shot XUV continua combining polarization gating, ionization gating, and trajectory selection with suitable phase matching [12].

In our previous work [13], we proposed a scheme to generate isolated sub-100-as pulses with 30 fs lasers combining the polarization gating technique and optimizing the parameters

of two-color lasers. Only one control field modulates the ellipticity and the amplitude of the driving field simultaneously and the limitation of the duration of the driving field is about 30 fs. Here, to make our scheme adapt to longer-duration driving pulses, we use two control fields to modulate the ellipticity and amplitude of the driving field separately in two directions. By optimizing the laser fields, an isolated 100 as pulse is generated.

II. THEORETICAL DETAILS

In our simulation, a 50 fs, 800 nm field acts as the driving field and the control fields are a 50 fs, 1550 nm field and a 50 fs, 1200 nm field. The synthesized three-color field can be expressed as:

$$\begin{aligned} \vec{E}_s = & E_1 \exp[-2 \ln(2)t^2/\tau_1^2] \cos(\omega_1 t + \phi_1) \vec{x} \\ & + E_2 \exp\{-[2 \ln(2)(t + t_2)^2/\tau_2^2]\} \cos[\omega_2(t + t_2) + \phi_2] \vec{x} \\ & + E_3 \exp[-2 \ln(2)(t + t_3)^2/\tau_3^2] \cos[\omega_3(t + t_3) + \phi_3] \vec{y}, \end{aligned} \quad (1)$$

where E_1 , E_2 and E_3 are the amplitudes of the electric fields of the driving and the control fields, ω_1 , ω_2 and ω_3 (τ_1 , τ_2 and τ_3) are the frequencies [the pulse durations in full width at half maximum (FWHM)] of the driving and the control fields, t_2 and t_3 define the time delays between the driving and the control fields, and ϕ_1 , ϕ_2 and ϕ_3 are the CEPs of the driving and the control fields. I_1 , I_2 and I_3 are the intensities of the driving and the control fields. Here we set $\tau_1 = \tau_2 = \tau_3 = 50$ fs, $I_1 = 5 \times 10^{14}$ W/cm², $I_2 = I_3 = 5 \times 10^{13}$ W/cm², $\phi = 0$, t_2 and t_3 are optimized to approach an intense supercontinuum.

The principle of the experimental scheme is shown in Fig. 1. A linearly polarized input beam is split by beam splitter 1 (BS1), one beam goes through the flat mirror M1 and acts as the driving field. The other beam is split once again by beam splitter 2 (BS2), and the two beams go through optical parametric amplifier 1 (OPA1) and OPA2 respectively acting as two control fields. A half-wave plate (HWP) is used to rotate the polarization of one beam.

As we explained in our previous paper [13], in HHG, only those electrons born at time t_b and that return to their parent ions at time t in the same position will emit XUV radiation. Here, t_b and t must synchronously satisfy the following two

*xfchen@sjtu.edu.cn

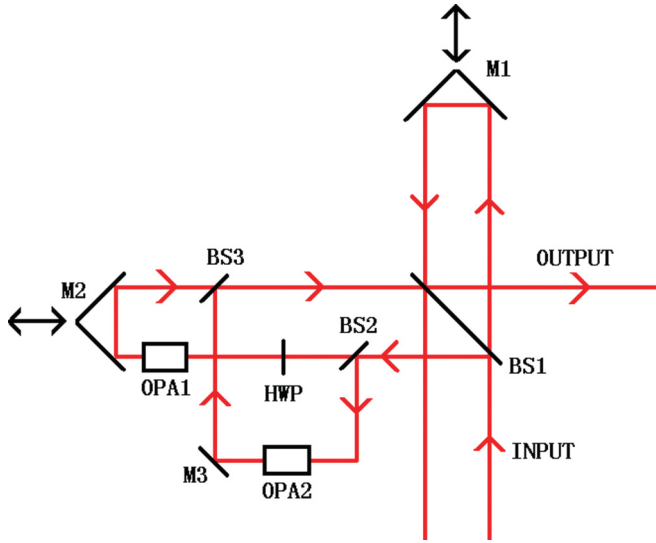


FIG. 1. (Color online) Principle of the experimental scheme. M1–M3 are flat mirrors (M1 and M2 could be adjusted), BS1–BS3 are beam splitters, OPA1 and OPA2 are optical parametric amplifiers, and HWP is a half-wave plate.

equations:

$$\int_{t_b}^t \left(\int_{t_b}^t \vec{E}_s(t) \vec{x} dt \right) dt = 0, \quad (2)$$

$$\int_{t_b}^t \left(\int_{t_b}^t \vec{E}_s(t) \vec{y} dt \right) dt = 0. \quad (3)$$

Each pair of such t_b and t defines a quantum path [13]. On the other hand, if one or both of Eqs. (2) and (3) cannot be satisfied, the ionized electron will never return to its parent ion and generate HHG. In our scheme, we try to realize quantum-path control by using two control fields to modulate the ellipticity and amplitude of the driving field. Through reshaping $\vec{E}_s(t)$ by optimizing the parameters of the two control fields, we select some quantum path by satisfying Eqs. (2) and (3) and meanwhile destroy other paths by destroying Eqs. (2) and (3). In this way, isolated ultrashort pulses can be generated.

III. RESULTS AND DISCUSSION

First, to find the optimal value of t_3 , we temporarily let $E_2 = 0$. For the driving field alone, limited by Eq. (2), electrons form three dominant quantum paths marked R1, R2, and R3 [14] as shown in Fig. 2 (red lines with arrows). After the control field (E_3) is included, three paths will be selected once again through Eq. (3). The synthesized field and its ellipticity are shown in Fig. 2 (black dashed line for the electric field of the synthesized field in the x direction, blue dotted line for the electric field in the y direction, and green solid line for its ellipticity). The maximum of ellipticity is 1, corresponding to a circularly polarized field, and the minimum is 0, corresponding to a linearly polarized field. With lower ellipticity, the linearly polarization is better. As shown in Fig. 2, if we set the time delay between the driving and the control field $t_3 = 1.5\pi/\omega_3 - 0.5\pi/\omega_1$, quantum paths R1 and R3 pass through two peaks of the ellipticity curve, respectively, where the electric field in the

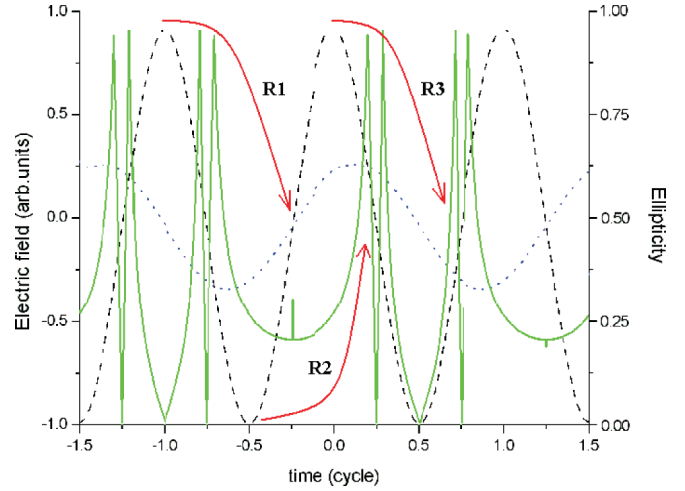


FIG. 2. (Color online) Electric field of the synthesized field in x direction (black dashed line), electric field in y direction (blue dotted line), and its ellipticity (green solid line); three dominant quantum paths (red lines with arrow).

x direction is close to zero and the electric field in y direction is large while quantum path R2 just passes through one trough. The result is that R2 remains while R1 and R3 are destroyed. Thus, we fix $t_3 = 1.5\pi/\omega_3 - 0.5\pi/\omega_1$ in the following.

On the other hand, we calculate the kinetic energy in the x direction as

$$E_{\text{kin}x}(t) = \frac{1}{2} \max \left\{ \left[\int_{t_b}^t E_{sx}(t) dt \right]^2 \right\},$$

in which t_b and t satisfy Eqs. (2) and (3) or else $E_{\text{kin}x}(t) = 0$ as shown in Fig. 3(a) for the driving field alone and in Fig. 3(c) for the synthesized field. We see three peaks (A, B, and C) corresponding to three quantum paths (R1, R2, and R3 in Fig. 2), respectively in Fig. 3(a). Each peak represents one quantum path; the left and the right arms represent the short

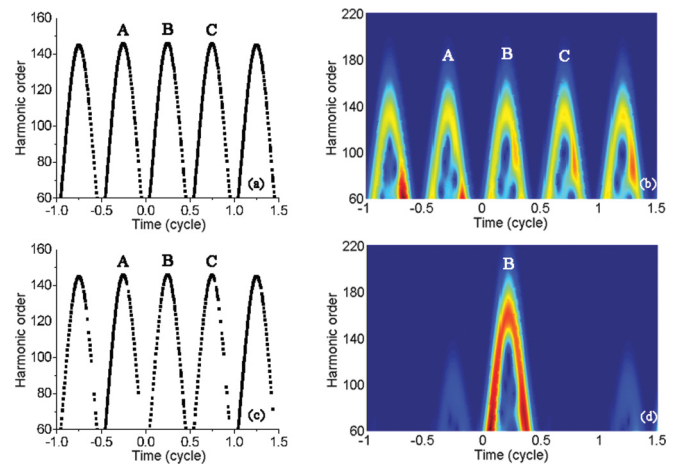


FIG. 3. (Color online) (a) Dependence of kinetic energy in x direction on the recombination times for the driving field alone. (b) Time-frequency diagram of the HHG in x direction for driving field alone. (c) Dependence of kinetic energy in x direction on recombination times for synthesized field. (d) Time-frequency diagram of the HHG in x direction for the synthesized field.

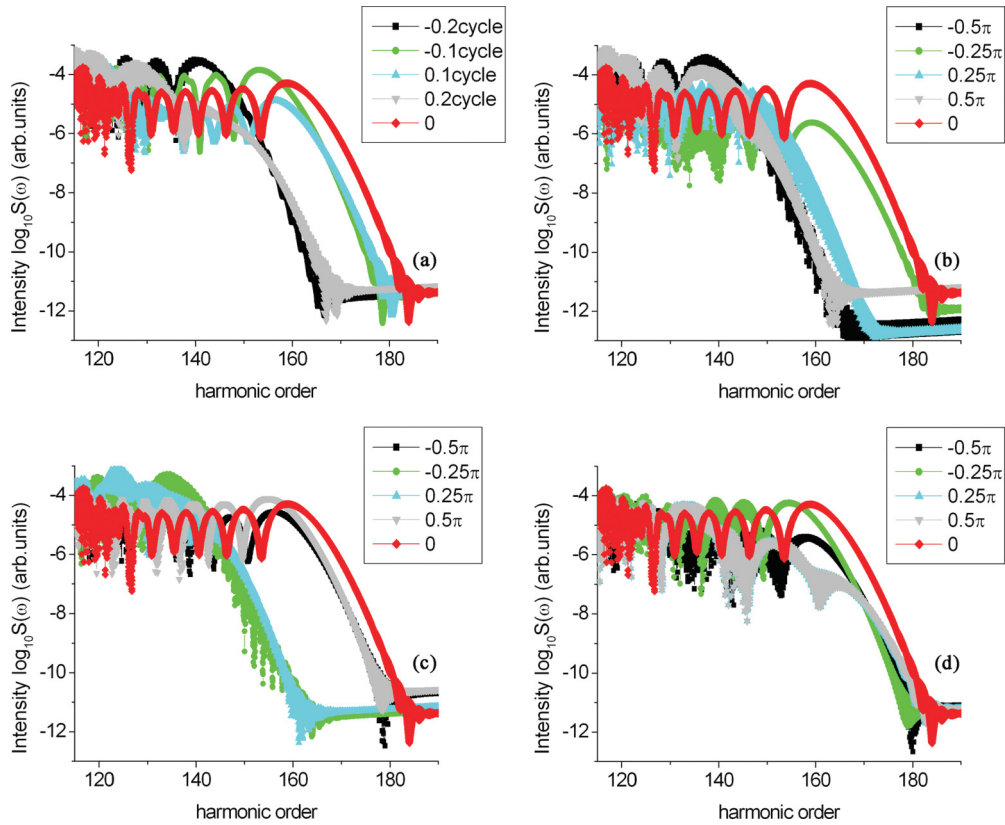


FIG. 4. (Color online) (a) Harmonic spectra with different time delay t_2 (red diamonds, gray nablas, cyan triangles, green circles, and black squares for $t_2 = 0, 0.2, 0.1, -0.1$, and -0.2 cycle of driving field, respectively). (b) Harmonic spectra with different CEPs of the driving field E_1 (red diamonds, gray nablas, cyan triangles, green circles, and black squares for $\phi_1 = 0, 0.5\pi, 0.25\pi, -0.25\pi$, and -0.5π , respectively). (c) Harmonic spectra with different CEPs of the control field E_2 (red diamonds, gray nablas, cyan triangles, green circles, and black squares for $\phi_2 = 0, 0.5\pi, 0.25\pi, -0.25\pi, -0.5\pi$, respectively). (d) Harmonic spectra with different CEPs of the control field E_3 (red diamonds, gray nablas, cyan triangles, green circles, and black squares for $\phi_3 = 0, 0.5\pi, 0.25\pi, -0.25\pi$, and -0.5π , respectively).

and the long electron trajectories, respectively. The influence brought by the control field (E_3) is clearly shown in Fig. 3(c), compared with the driving field alone [Fig. 3(a)]. All quantum paths except B have been reconstructed to some extent. The time-frequency analyses of the XUV spectra in the x direction is shown in Fig. 3(b) for the driving field alone and in Fig. 3(d) for the synthesized field. We find that Figs. 3(b) and 3(d) match Figs. 3(a) and 3(c) quite well: all quantum paths are destroyed except B.

Second, we recover E_2 and try to optimize t_2 to gain an isolated ultrashort pulse. The HHG spectra for the synthesized three-color field with different time delay t_2 are shown in Fig. 4(a) (red diamonds, gray nablas, cyan triangles, green circles, and black squares for $t_2 = 0, 0.2, 0.1, -0.1$, and -0.2 cycle of the driving field, respectively). We find that an XUV supercontinuum (about 70 eV) appears [red diamonds in Fig. 4(a)]. The influence of the CEPs of the driving and the control fields are shown in Fig. 4(b) (red diamonds, gray

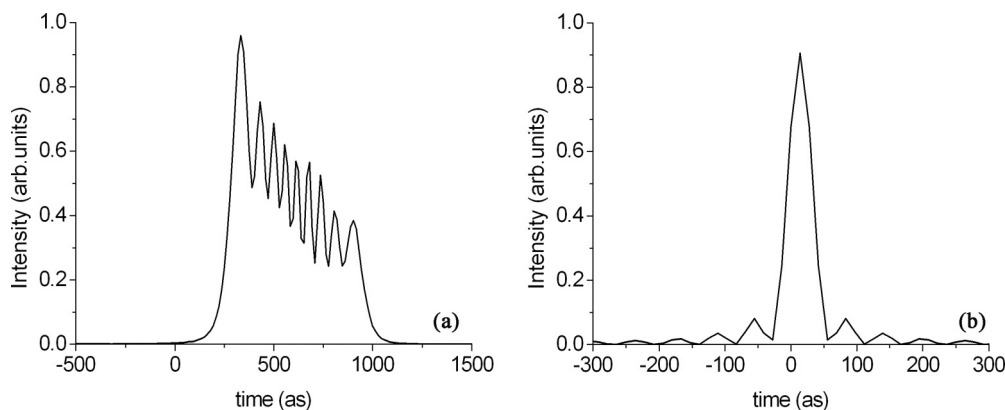


FIG. 5. (a) Temporal profile of single XUV pulse generated in synthesized three-color field without phase compensation. (b) Temporal profile of single XUV pulse generated in synthesized three-color field with phase compensation.

nablas, cyan triangles, green circles, and black squares for $\phi_1 = 0, 0.5\pi, 0.25\pi, -0.25\pi$, and -0.5π , respectively), Fig. 4(c) (red diamonds, gray nablas, cyan triangles, green circles, and black squares for $\phi_2 = 0, 0.5\pi, 0.25\pi, -0.25\pi$, and -0.5π , respectively), and Fig. 4(d) (red diamonds, gray nablas, cyan triangles, green circles, and black squares for $\phi_3 = 0, 0.5\pi, 0.25\pi, -0.25\pi$, and -0.5π respectively). We see that the supercontinuum strongly depends on the stable CEPs of the driving and the control fields.

The temporal profile of the as pulse supported by the supercontinuum (red diamonds in Fig. 4) is calculated by a simple inverse Fourier transformation of the XUV supercontinuum, which gives an isolated 100 as pulse without phase compensation, as shown in Fig. 5(a). With proper phase compensation, the duration of the XUV pulse becomes as short as 40 as and is shown in Fig. 5(b).

IV. CONCLUSION

In conclusion, we have improved upon our earlier scheme to generate intense isolated as pulses with many-cycle high-

power laser fields. We use two control fields to modulate the ellipticity and amplitude of the driving field independently, and the limitation of the duration of the driving field is enlarged to 50 fs. We optimize the time delay between the driving field and the control fields to produce isolated ultrashort pulses. With proper time delays, we reach a long XUV supercontinuum which supports an isolated ultrashort 100 as pulse. We believe our theoretical model gives better “ultrashort probes” and could be applied in practice for detecting and controlling ultrafast processes.

ACKNOWLEDGMENTS

This research was supported by the National Natural Science Foundation of China (Grant No. 1073408061078009), the National Basic Research Program “973” of China (Grant No. 2011CB808101), the Foundation for Development of Science and Technology of Shanghai (Grant No. 11XD1402600), and the Open Fund of the State Key Laboratory of High Field Laser Physics.

-
- [1] P. B. Corkum and F. Krausz, *Nat. Phys.* **3**, 381 (2007).
 - [2] M. Drescher, M. Hentschel, R. Kienberger, M. Uiberacker, V. Yakovlev, A. Scrinzi, Th. Westerwalbesloh, U. Kleineberg, U. Heinzmann, and F. Krausz, *Nature (London)* **419**, 803 (2002).
 - [3] P. Tzallas, E. Skantzakis, C. Kalpouzos, E. P. Benis, G. D. Tsakiris, and D. Charalambidis, *Nat. Phys.* **3**, 846 (2007).
 - [4] Juan J. Carrera, X. M. Tong, and Shih-I Chu, *Phys. Rev. A* **74**, 023404 (2006).
 - [5] P. B. Corkum, *Phys. Rev. Lett.* **71**, 1994 (1993).
 - [6] M. Lewenstein, Ph. Balcou, M. Yu. Ivanov, Anne L’Huillier, and P. B. Corkum, *Phys. Rev. A* **49**, 2117 (1994).
 - [7] C. A. Haworth, L. E. Chipperfield, J. S. Robinson, P. L. Knight, J. P. Marangous, and J. W. G. Tisch, *Nat. Phys.* **3**, 52 (2007).
 - [8] Xiaohong Song, Zhinan Zeng, Yuxi Fu, Bo Cai, Ruxin Li, Ya Cheng, and Zhizhan Xu, *Phys. Rev. A* **76**, 043830 (2007).
 - [9] I. J. Sola, E. Mevel, L. Elouga, E. Constant, V. Strelkov, L. Poletto, P. Villoresi, E. Benedetti, J.-P. Caumes, S. Stagira, C. Vozzi, G. Sansone, and M. Nisoli, *Nat. Phys.* **2**, 319 (2006).
 - [10] E. Gouliemakis, M. Schultze, M. Hofstetter, V. S. Yakovlev, J. Gagnon, M. Uiberacker, A. L. Aquila, E. M. Gullikson, D. T. Attwood, R. Kienberger, F. Krausz, and U. Kleineberg, *Science* **320**, 1614 (2008).
 - [11] Carlo Altucci, Rosario Esposito, Valer Tosa, and Raffaele Velotta, *Opt. Lett.* **33**, 2943 (2008).
 - [12] Carlo Altucci, Raffaele Velotta, Valer Tosa, Paolo Villoresi, Fabio Frassetto, Luca Poletto, Caterina Vozzi, Francesca Calegari, Matteo Negro, Sandro De Silvestri, and Salvatore Stagira, *Opt. Lett.* **35**, 2798 (2010).
 - [13] Songsong Tang and Xianfeng Chen, *Phys. Rev. A* **82**, 013827 (2010).
 - [14] Weiyi Hong, Peixiang Lu, Pengfei Lan, Zhenyu Yang, Yuhua Li, and Qing Liao, *Phys. Rev. A* **77**, 033410 (2008).